



Molecular size- and shape-selective Knoevenagel condensation over microporous Cu₃(BTC)₂ immobilized amino-functionalized basic ionic liquid catalyst

Qun-xing Luo ^a, Xue-dan Song ^a, Min Ji ^{a,*}, Sang-Eon Park ^b, Ce Hao ^a, Yan-qin Li ^a

^a School of Chemistry, Faculty of Chemical, Environmental and Biological Science and Technology, Dalian University of Technology, Dalian 116023, People's Republic of China

^b Laboratory of Nano-Green Catalysis and Nano Center for Fine Chemicals Fusion Technology, Department of Chemistry, Inha University, Incheon 402-751, Republic of Korea



ARTICLE INFO

Article history:

Received 24 February 2014

Received in revised form 27 March 2014

Accepted 29 March 2014

Available online 8 April 2014

Keywords:

Size and shape-selective catalysis

Metal-organic framework

Cu₃(BTC)₂ nanocavities

Amino-functionalized basic ionic liquid

Immobilization

ABSTRACT

A novel molecular size- and shape-selective catalyst, microporous metal-organic framework HKUST-1 immobilized amino-functionalized basic ionic liquid (ABIL-OH), was synthesized by facile impregnation and activation. Characterizations and catalytic results revealed that the catalytically active species ABIL-OH could be confined in well-defined HKUST-1 nanocavities via Cu–NH₂ coordination bond. The resulting ABIL-OH/HKUST-1 heterogeneous catalyst showed comparable catalytic activity and enhanced selectivity in liquid phase Knoevenagel condensation, and it could be recovered conveniently and reused at least 5 times without significant loss of its catalytic efficiency. Moreover, ABIL-OH/HKUST-1 catalyst demonstrated distinct size- and shape-selective properties for discrimination of reactants in Knoevenagel condensation. It was supposed that diffusion kinetics of reactants might be controlling step and play a more important role than the nature of the substituents in the confined microenvironment.

© 2014 Elsevier B.V. All rights reserved.

1. Introduction

Molecular size- and shape-selective catalysis is a significant and fascinating concept in the field of heterogeneous catalysis. It is widely applied to produce target compounds with high selectivity. This characteristic catalysis is based on the sizes and shapes of substrate molecules in comparison with the windows and channels of nanoporous materials [1,2]. The traditional porous zeolites have been investigated extensively and have achieved a few groundbreaking successes [3–5]. Nevertheless, the available pore size of zeolites are usually small (below 1 nm) and difficult to be tailored. These inherent imperfections hinder application of zeolites in liquid phase reactions where the substrates are relatively large. Consequently, extending the size and shape-selective catalysis to other nanoporous materials with larger pore sizes is highly desired.

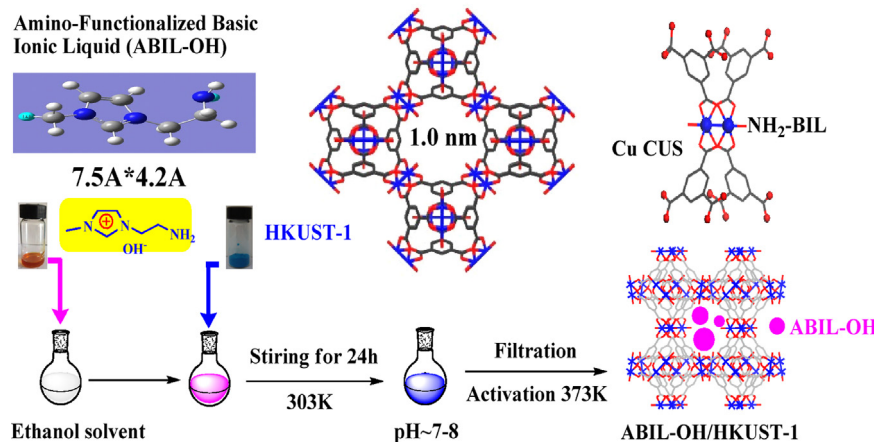
In recent years, metal-organic frameworks (MOFs) or porous coordination polymers (PCPs) can be considered as promising complementing in expanding the molecular size and shape-selective catalysis [6–8]. Compared with zeolites, the extra-large surface

areas, exceptional porosity and tunability of pore structure offer unprecedented possibilities for MOFs to host catalytically active guest molecules by post-synthetic modification strategy (PSM) [9,10]. During the past decade, several catalytically active guest species like metal nanoparticles [11,12], polyoxometalates [13,14], organo-metallics [15,16] and biomimetic species [17] have been successfully incorporated inside MOFs. Among various types of MOFs, the well-known copper-based MOFs [Cu₃(BTC)₂] (HKUST-1) (BTC = 1,3,5-benzenetricarboxylate) has been intensively studied. HKUST-1 has a three dimensional square-shaped channel system (1.0 nm × 1.0 nm) and accessible nanocavities [18]. Interestingly, the coordinatively unsaturated Cu²⁺ sites (CUS) are homogeneously distributed in the HKUST-1 framework, which would provide a feasible concept to develop novel functionalized materials by surface decoration with electron rich functional group (NH₃, pyridine and organic amine) [19,20].

The liquid-phase Knoevenagel condensation between an active methylene compound and a carbonyl group (C=O) is a very useful C–C bond coupling reaction to prepare several important chemical intermediates. In general, organic bases (alkylamine and ammonium salts) [21,22] or Lewis acid catalysts [23] under homogeneous system could effectively catalyze this reaction, but their utilization is associated with the work-up of the reaction mixture and the

* Corresponding author. Tel.: +86 411 84986329; fax: +86 411 84986329.

E-mail address: jimin@dlut.edu.cn (M. Ji).



Scheme 1. The schematic illustration for synthesizing ABIL-OH/HKUST-1 catalyst.

generation of considerable amounts of liquid waste. For this reason, although several alternative heterogeneous catalysts have been successfully applied in Knoevenagel condensation, such as zeolites [24], mesoporous carbon nitride [25], organic-functionalized mesoporous silicon [26] and MOFs materials [27–29], it usually requires high reaction temperature or microwave irradiation. More recently, task-specific ionic liquids (TSILs) as environmentally benign solvent and/or co-catalyst have demonstrated excellent catalytic performance in Knoevenagel condensation [30,31]. Unfortunately, the homogeneous catalysis or liquid–liquid biphasic system using TSILs as catalyst could not address problem in separation and recycling of catalyst. On the other hand, the reaction mixture usually contains inevitably some byproducts from the consecutive reaction of the primary product over the homogeneous catalyst.

In this regard, supported ionic liquid catalysis (SILC) might be an effective method to solve these major drawbacks. The novel SILC would be likely to inspire distinct catalytic performance due to combination the advantages of TSILs organocatalyst with those of heterogeneous support [32–34]. Recently, the viability of this concept has been confirmed by several investigations. Xia and co-workers [35,36] reported hydroxyapatite-encapsulated γ -Fe₂O₃ supported diethyl aliphatic amine basic ionic liquids, and this magnetic catalyst could be easily isolated from the reaction mixture by simple magnetic decantation and reused four times without significant degradation. Hardacre et al. [37] prepared silica supported basic ionic liquid catalyst that showed excellent recyclability in Knoevenagel condensation. In addition, other solid supports like silica-based materials (SiO₂, SBA-15, MCM-41) [38–40], organic polymers [41], carbon material (CNTs) [42,43] supported ionic liquids catalyst by covalent or non-covalent attachment have also been investigated in a variety of catalytic reactions. However, there have been a handful of attempts on the investigation of metal-organic framework supported ionic liquid.

Very recently, our group, for the first time, reported Brønsted acidic ionic liquid-functionalized MIL-101 as a heterogeneous acid catalyst for the acetalization of benzaldehyde with glycol. The catalyst showed higher catalytic performance than its homogeneous counterpart with excellent reusability [44]. Jhung and co-workers reported MIL-101 supported 1-butyl-3-methylimidazolium chloride ionic liquid for adsorptive desulfurization from liquid fuel [45]. In this contribution, we reported a facile method to prepare micro-porous HKUST-1 immobilized amino-functionalized basic ionic liquid organocatalyst. This novel ABIL-OH/HKUST-1 heterogeneous catalyst did not only exhibit remarkable catalytic performance and recyclability, but also showed distinct size- and shape-selective catalysis in Knoevenagel condensation.

2. Materials and methods

2.1. Materials

Toluene was dried with 5A molecular sieve. Other Reagents were used without further purification. Cupric nitrate trihydrate ($\text{Cu}(\text{NO}_3)_2 \cdot 3\text{H}_2\text{O}$), sodium hydroxide, 1-methylimidazole (99%), acetonitrile, toluene and ethanol were purchased from Sinopharm Chemical Reagent Co., Ltd. or Tianjin Kemiou Chemical Reagent Co., Ltd.

Other reagents were purchased from the following distributors:

1,3,5-Benzenetricarboxylic acid (H_3BTC , 99%): Meryer Chemical Technology Co., Ltd.

2-Bromoethylamine hydrobromide (99%): J&K Scientific.

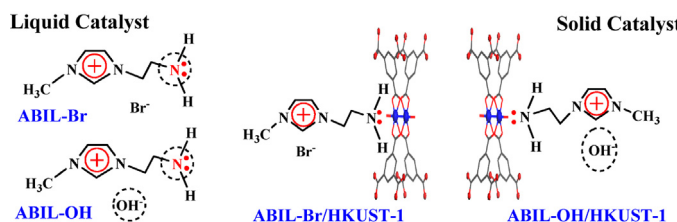
2.2. Preparation of metal-organic framework materials

Metal-organic framework HKUST-1 crystals were prepared by a solvothermal reaction [18]. Typically, $\text{Cu}(\text{NO}_3)_2 \cdot 3\text{H}_2\text{O}$ (4.5 mmol, 1.087 g) was dissolved in 15 mL deionized water and then mixed with H_3BTC (2.5 mmol, 0.525 g) dissolved in 15 mL ethanol. The mixture was stirred for 30–60 min, and then transferred to a 50 mL Teflon autoclave liner and sealed to heat at 120 °C for 12 h. The obtained blue powder was filtered and washed several times with deionized water and ethanol, and then dried in vacuum overnight at 150 °C. MIL-101 material was provided by our previous synthesis ($S_{\text{BET}} = 1873 \text{ m}^2 \text{ g}^{-1}$, $V_{\text{total}} = 0.906 \text{ cm}^3 \text{ g}^{-1}$) [44].

2.3. Preparation of amino-functionalized basic ionic liquid (ABIL-OH)

The amino-functionalized basic ionic liquid (ABIL-OH) was prepared according to the literature, as illustrated in Scheme S1 [46,47]. Methylimidazole (4.15 g, 0.05 mol) and 2-bromoethylamine hydrobromide (10.24 g, 0.05 mol) were dissolved in 50 mL acetonitrile at 80 °C for 24 h under nitrogen atmosphere with stirring. On completion, the solvent was removed by rotary evaporation, and the residue was washed with ethanol (3 × 10 ml). The solid residue was dissolved in water. Then the pH value of the solution was adjusted to 8 by the addition of sodium hydroxide. The obtained solution was concentrated by rotary evaporation and the product 1 (ABIL-Br) was obtained.

During anion metathesis, the obtained product 1 and sodium hydroxide (2 g, 0.05 mol) were added into ethanol–water (v/v, 1:1, 15.0 ml), and then the mixture was stirred for 24 h at ambient



Scheme 2. The structural model of different catalyst.

temperature (30 °C). The upper suspension was extracted to remove the precipitated bromide salt and the organic phase was concentrated, and the product 2 was obtained.

2.4. Catalyst preparation

The catalyst was prepared by a facile impregnation and activation, as illustrated in **Scheme 1**. In a round bottom flask, 0.3 g ABIL-OH or ABIL-Br was dissolved in 25 ml ethanol solvent, respectively. Metal-organic framework material (0.5 g) was suspended in solution above, and the mixture was stirred at ambient temperature (30 °C) for 24 h with magnetic stirring. The solvent was separated by filtration and excess of amino-functionalized ionic liquid was removed by washing with DMF (3 × 10 ml) and ethanol (3 × 10 ml). The synthesized heterogeneous catalysts were termed ABIL-OH/HKUST-1 and ABIL-Br/HKUST-1. Finally, the catalysts were dried under vacuum at 80 °C for 12 h. The structural model of catalyst was shown in **Scheme 2**.

2.5. General procedure for Knoevenagel condensation

Knoevenagel condensation of aromatic aldehydes with malononitrile was carried out in self-made glass microreactor under batch reaction conditions (**Scheme 3**). In a typical experiment, 2 ml toluene, 2 mmol aromatic aldehydes, 4 mmol malononitrile, 50 mg catalysts were placed into a magnetically stirred glass reactor under ambient temperature (30 °C). When the reaction was completed, the product of Knoevenagel condensation was separated by centrifugation. The catalytic activity and selectivity were determined by GC-MC (Agilent 6890, HP-5 capillary column 25 m, 0.32 mm).

2.6. Reusability of catalyst and the hot filtration test

After every reaction, the catalysts were washed with toluene (2 × 5 ml) and dried at 80 °C for 2 h, and reused in a subsequent reaction under identical condition. The hot filtration test was carried out by stopping a standard reaction after 30 min. The reaction mixture was separated from the suspended catalyst. The liquid phase was then transferred to another flask and again allowed to react.

2.7. Molecular simulation and calculation of substrates dimension

The ground state geometric optimizations of all molecules were performed with the density functional theory (DFT) method through Gaussian 09 program suites. We employed the B3LYP functional in Gaussian 09 and the relativistic effects were taken into account by using the 6-311G basis sets for the simulation.

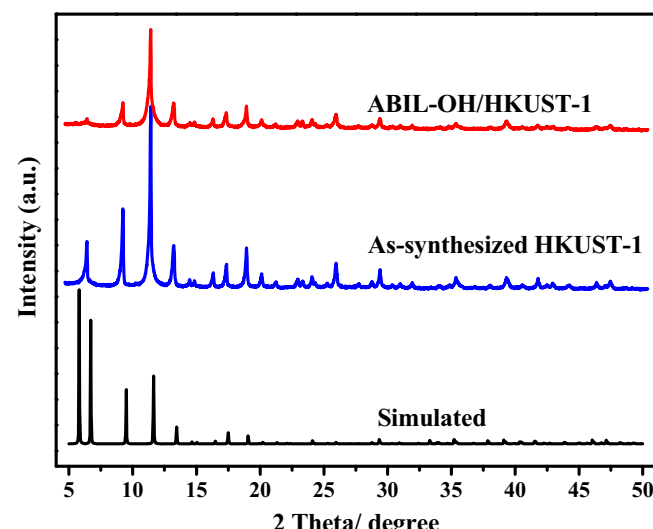


Fig. 1. Powder X-ray diffraction (PXRD) patterns of ABIL-OH/HKUST-1 catalyst and as-synthesized HKUST-1 sample.

2.8. Characterization techniques

The Powder X-ray diffraction (PXRD) data was recorded on a Rigaku diffractometer (D/MAX-IIIa, 3 kW) using Cu K α radiation, scanning angle from 5° to 50°. The nitrogen adsorption-desorption was performed at 77 K using a Quantachrome AUTOSORB 1C apparatus. Before the analysis, the samples were evacuated at 150 °C for 12 h. Fourier transform infrared (FT-IR) spectroscopy was performed on Bruker-Tensor 27 infrared spectrometer in the range 400–4000 cm⁻¹ using KBr pellets. DRS UV-vis spectroscopy was performed on Agilent Cary 5000 spectrophotometer. Scanning electron microscopy images (SEM) and energy dispersive analysis of X-ray (EDX) were obtained on JSM-5600LV instrument. X-ray photoelectron spectroscopy (XPS) was recorded using Al K Alpha source. Thermogravimetric analysis (TGA) was carried out on TA instrument from room temperature to 800 °C with a heating rate of 10 °C min⁻¹ under a flow of N₂. Elemental analysis (EA) was performed on vario EL III.

3. Results and discussions

3.1. Catalyst characterization

3.1.1. Powder X-ray diffraction (PXRD)

For synthesized ABIL-OH/HKUST-1 catalyst, initial evidence of intrinsic crystalline structures was confirmed by Powder X-ray diffraction, as shown in **Fig. 1**. The PXRD patterns of ABIL-OH/HKUST-1 catalyst show that almost all the main diffraction peaks are observed in accordance with simulated pattern and as-synthesized HKUST-1 sample, apart from some slight variations in the Bragg intensities. These results clearly indicate that the crystalline structure of HKUST-1 is unchanged and intact during the synthetic process.



Scheme 3. Knoevenagel condensation of aromatic aldehyde with malononitrile under ambient temperature (30 °C).

Table 1

The physical and chemical properties of all samples.

Sample	Textural properties ^a		Cu ^b (%)	Loading amount of ABIL-OH/mmol g ^{-1c}
	S _{BET} /m ² g ⁻¹	V _{total} /cm ³ g ⁻¹		
As-synthesized HKUST-1	1158	0.50	9.0	–
ABIL-OH/HKUST-1	338	0.21	6.6	1.07

^a The N₂ physical adsorption–desorption at 77 K.

^b SEM-EDX.

^c Measured by elemental analysis, nitrogen content = 3.21 mmol g⁻¹.

3.1.2. Scanning electron microscopy (SEM-EDX)

The surface morphology and chemical composition of all samples were characterized by SEM-EDX (Fig. S1). The as-synthesized HKUST-1 sample is octahedral crystal morphology with smooth surface, and particles size is about 20–25 μm. The Cu content is 9.0% by EDX analysis. The surface of ABIL-OH/HKUST-1 catalyst tends to be rough, but the octahedral crystal morphology is still observed. Meanwhile, particle size of octahedral crystallites could remain the same (20–25 μm). The corresponding Cu content decreases to 6.6% (Table 1) which could be attributed to a handful leaching of transition metal Cu ions from framework under weak alkaline solution.

3.1.3. N₂ physical adsorption–desorption

The N₂ adsorption–desorption isotherms of all samples were exhibited in Fig. S2. Compared with the as-synthesized HKUST-1 sample, the ABIL-OH/HKUST-1 catalyst shows a significant decrease in the adsorbed N₂ amount. The as-synthesized HKUST-1 shows a BET surface area and a total pore volume of 1158 m² g⁻¹ and 0.50 cm³ g⁻¹, whereas ABIL-OH/HKUST-1 catalyst has corresponding values of 338 m² g⁻¹ and 0.21 cm³ g⁻¹. Additionally, the N₂ adsorption–desorption curve of ABIL-OH/HKUST-1 catalyst shows I/IV mixed type isotherm with H₂ hysteresis loop, which is indicative of existing microporous and mesoporous structures. The pore size distribution curves are obtained by using the methods of Density Functional Theory (DFT), as shown in Fig. S2. The formed mesoporosity is usually ascribed to stacking of nanoparticles. It is worthwhile to note that microporous size decreased from 1.1 nm to 0.8 nm and 0.6 nm, which could be attributed to the incorporation of ABIL-OH organocatalyst inside HKUST-1 nanocavities.

3.1.4. FT-IR spectroscopy

FT-IR spectra of all samples were shown in Fig. 2. Compared with as-synthesized HKUST-1, the presence of new bands in high

wavenumbers region over ABIL-OH/HKUST-1 catalyst is observed. The characteristic peak at 3149 cm⁻¹ is due to sp² C–H stretching vibrations of imidazole moiety. The band at 2962 cm⁻¹ and 2875 cm⁻¹ are assigned to aliphatic C–H asymmetric and symmetrical stretching vibrations of alkyl chain. In the low wavenumbers region, the peak at 1569 cm⁻¹ and 1643 cm⁻¹ can be ascribed to the C=C and C=N vibrations of the imidazole ring. The band at 1109 cm⁻¹ is assigned to the C–C skeleton stretching vibration of alkyl chain. Moreover, two important peaks at 837 cm⁻¹ and 1109 cm⁻¹ are observed, which could be attributed to N–H out-of-plane bending vibration and C–N stretching vibration of amino-alkyl chain [38,39]. It is interesting to note that the wavenumber of N–H out-of-plane bending vibration is shifted to lower values (808 cm⁻¹), which is tentatively ascribed to interaction (coordination bond N–Cu) between –NH₂ and coordinatively unsaturated metal sites Cu(II) in HKUST-1 frameworks.

3.1.5. DRS UV-vis spectra

Since bivalent copper species Cu²⁺ (3d⁹) presents in HKUST-1 framework, it would involve d–d transitions in changed local coordination environment of central Cu²⁺ ion in electronic spectra analysis. Fully hydrated sample shows a azure color. Upon activation (dehydration), its color changes drastically into dark blue. However, ABIL-OH/HKUST-1 catalyst exhibits pale blue color (Fig. 3. Inset image A, B and C). This behavior reflects unequivocally the change in the close surrounding of copper species as the color is associated with d–d transitions of Cu²⁺ ions. The corresponding DRS UV-vis spectra are illustrated in Fig. 5. All samples demonstrate an edge around 350 nm due to a ligand to metal charge transfer (LMCT) transition from oxygen to copper atoms (O → Cu). In addition, it is obvious to observe that as-synthesized HKUST-1 (hydration) sample shows a band centered at 586 nm because of characteristic of

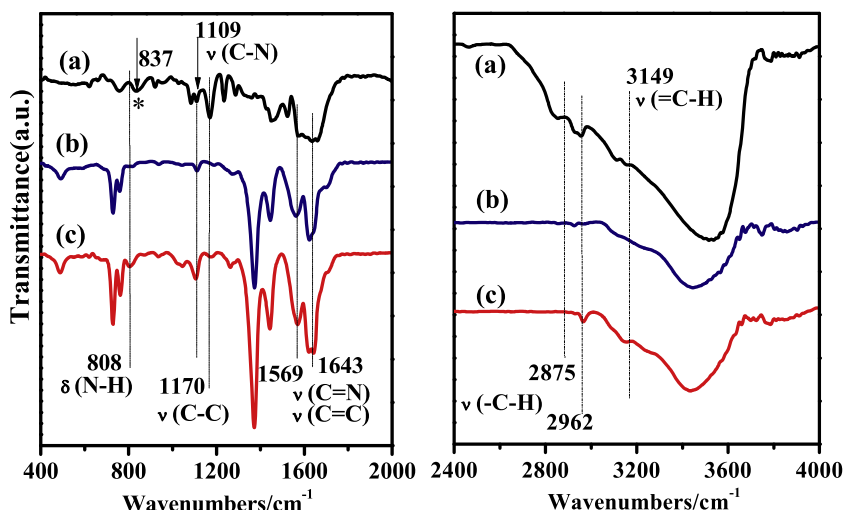


Fig. 2. Partial enlarged view of FT-IR spectra. Low wavenumber (left); high wavenumber (right). Amino-functionalized basic ionic liquid ABIL-OH (a); as-synthesized HKUST-1 (b); ABIL-OH/HKUST-1 (c).

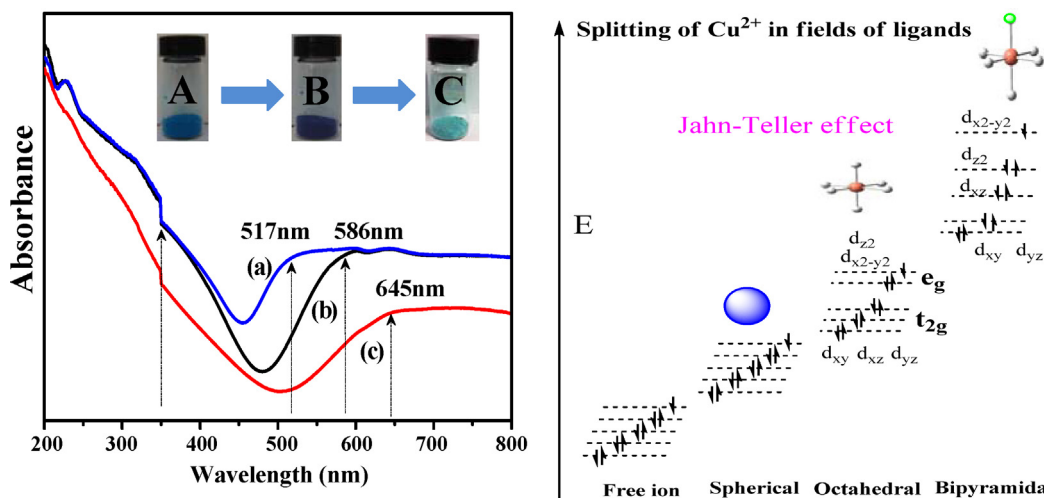


Fig. 3. The DRS UV-vis spectra of all samples (left) and splitting of bivalent copper species Cu²⁺ in the field of ligand in different coordination environments (right). Activated HKUST-1 (a); As-synthesized HKUST-1 (b); ABIL-OH/HKUST-1 (c).

the d-d transition for Cu(II) species in a distorted octahedral local geometry.

The distortion of octahedral complexes is commonly explained from the crystal field theory. Splitting of bivalent copper species Cu²⁺ in the field of ligand (Jahn-Teller effect) causing a distortion of the octahedral Cu²⁺ complex. The corresponding band of activated HKUST-1 is shifted to 517 nm due to removing of coordinated water. Interestingly, the spectrum tends to restore original state over ABIL-OH/HKUST-1 catalyst, apart from some extent red shift in the d-d band (~645 nm) [20,48,49]. One reasonable explanation for this phenomenon is that ABIL-OH molecules are re-adsorbed onto bivalent copper species Cu²⁺. This change in local coordination environment of central Cu²⁺ ion is sufficient to cause a visually color change.

3.1.6. X-ray photoelectron spectroscopy (XPS)

The X-ray photoelectron spectroscopy (XPS) was performed to investigate the surface characteristic (Fig. 4). The presence of new peak (BE at ~399 eV) in ABIL-OH/HKUST-1 catalyst is attributed to N 1s of the ABIL-OH group. The copper specie Cu 2p XPS spectrum of as-synthesized HKUST-1 is depicted around the range from 925 eV to 965 eV. Two characteristic peaks of Cu²⁺ are observed at 933.8 eV

and 953.5 eV, corresponding to Cu 2p_{3/2} and Cu 2p_{1/2}, respectively. Meanwhile, the well-known “shake-up satellite bands” (at the 938–946 eV and 961–965 eV regions) are observed [50–52]. However, it is worthwhile to note that the Cu 2p_{3/2} and Cu 2p_{1/2} bind energy of ABIL-OH/HKUST-1 catalyst shift from 933.8 eV to 933.3 eV and 953.5 eV to 953.0 eV, respectively. This slightly reduction of binding energy is because of Cu²⁺ center accepting the lone pair electrons from donating –NH₂ group. Additionally, the intensity of “shake-up satellite bands” is also decreased slightly. As a consequence, it is supposed that the coordination environment of Cu²⁺ center has changed slightly due to the interaction between the CUS and –NH₂ group.

3.1.7. Thermogravimetric analysis (TGA)

The thermogravimetric analysis (TGA) were also carried out from 30 °C to 800 °C with a heating rate of 10 °C min⁻¹ under N₂ flow, as depicted in Fig. 5. The TGA curve of as-synthesized HKUST-1 indicates an initial weight loss of about 22% up to 150 °C corresponding to the adsorbed water inner and outer surfaces of HKUST-1. However, ABIL-OH/HKUST-1 catalyst loses only ~7% weight at <150 °C because adsorption sites are occupied by ABIL-OH group. In the second step, there is about 23% weight loss at

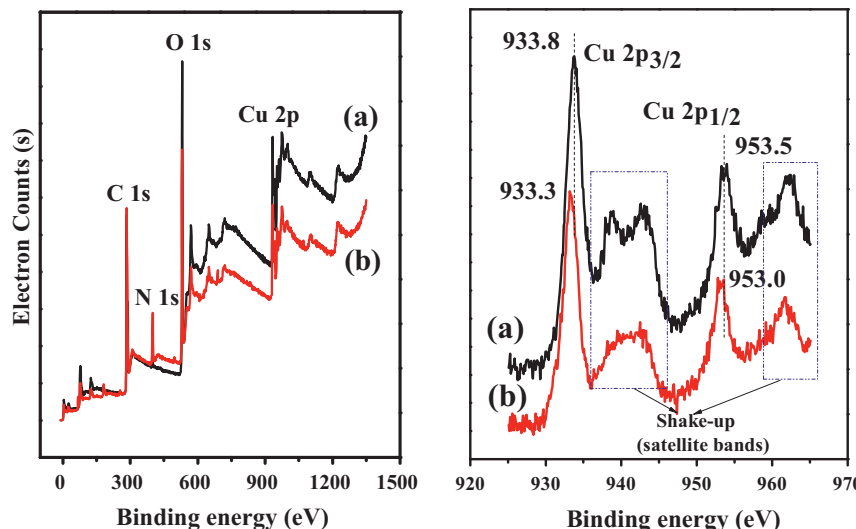


Fig. 4. X-ray photoelectron spectroscopy (XPS) of all samples. Survey XPS spectra (left); Cu 2p XPS spectra (right). As-synthesized HKUST-1 (a); ABIL-OH/HKUST-1 (b).

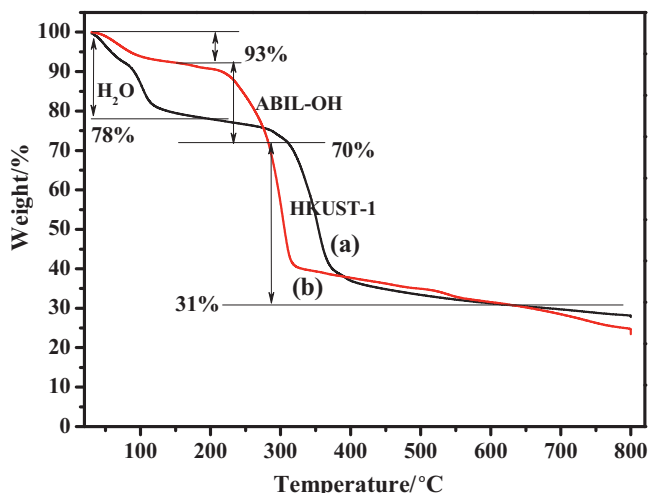


Fig. 5. The thermogravimetric analysis (TGA) curves of ABIL-OH/HKUST-1 catalyst and as-synthesized HKUST-1 sample. As-synthesized HKUST-1 (a); ABIL-OH/HKUST-1 (b).

150–290 °C, which is probably due to the decomposition of the ABIL-OH organocatalyst inside HKUST-1 nanocavities. Finally, the weight loss at ~300 °C is attributed to the complete collapse of HKUST-1 framework. In addition, the weight of residual solid ABIL-OH/HKUST-1 is lower than as-synthesized HKUST-1 sample. This result agrees with the previous observation from SEM-EDX analysis.

3.2. Catalytic performance

3.2.1. Catalytic activity study

As for synthesized ABIL-OH/HKUST-1 catalyst, the loading amount of ABIL-OH group is measured to be 1.07 mmol g⁻¹ by elemental analysis (Table 1). The catalytic performance was evaluated by using Knoevenagel condensation of benzaldehyde with malononitrile as a probe reaction under ambient temperature. Kinetic curves (dependence of conversion on reaction time) are depicted in Fig. 6. A blank experiment, Knoevenagel condensation cannot proceed in absence of catalyst. The as-synthesized HKUST-1 gives a maximum benzaldehyde conversion of ca. 55.3% after 240 min. Bracingly, ABIL-OH/HKUST-1 catalyst Exhibits 100% benzaldehyde conversion after 210 min. For the sake of

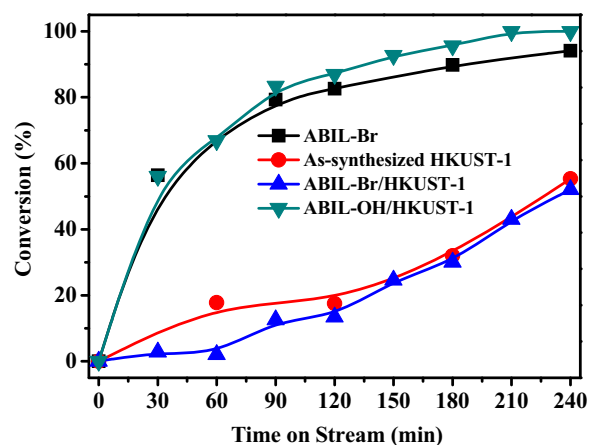


Fig. 7. Verification experiment of CUS-NH₂ interaction. Reaction condition: 2 ml toluene, 2 mmol benzaldehyde, 4 mmol malononitrile, reaction temperature = 30 °C, $m_{\text{cat}} = 50 \text{ mg}$ ABIL-OH/HKUST-1 or ABIL-Br/HKUST-1, 8 mg ABIL-OH or ABIL-Br, respectively.

comparison, homogeneous counterpart ABIL-OH organocatalyst was also examined under the same total number of OH⁻ active species. The employment of ABIL-OH organocatalyst presents admirable catalytic activity with 100% conversion only after 120 min. Nevertheless, it must be recognized that free —NH₂ group of ABIL-OH organocatalyst could serve as a Lewis basic site to make a contribution to the catalytic activity.

In order to further verify CUS-NH₂ interaction, homogeneous ABIL-Br organocatalyst and ABIL-Br/HKUST-1 heterogeneous catalysts were prepared and also evaluated under the same conditions, as depicted in Fig. 7. The ABIL-Br organocatalyst demonstrates high benzaldehyde conversion (94.1%) after 240 min because free —NH₂ group could serve as a Lewis basic site to catalyze Knoevenagel condensation. Nevertheless, ABIL-Br/HKUST-1 catalyst exhibits comparative catalytic activity with as-synthesized HKUST-1, but it is still lower than that of ABIL-Br and ABIL-OH/HKUST-1 catalysts. These results clearly indicate that lone pair electrons of free —NH₂ group interact with coordinatively unsaturated metal sites, and Lewis basic sites are shielded.

3.2.2. Recyclability and hot filtration tests

The recyclability of ABIL-OH/HKUST-1 catalyst was investigated under same reaction condition. After every reaction, the catalyst was washed with toluene and dried under vacuum. As shown in Fig. 8, it could maintain high catalytic activity (>90% conversion) and 100% selectivity after five times recycle, but the slightly decrease of conversion in continuing recycle of the reaction is observed. PXRD characterizations of fresh catalyst and reused catalyst were attempted to investigate the reason for the loss of the catalytic activity, as shown in Fig. S3. It is found that the main diffraction peaks of reused catalyst are observed, but several peaks at high angle region disappear. The reasonable interpretation for collapse of partial framework might be the reduction of Cu(II) in HKUST-1 framework by the aldehyde group of reactant [53,54]. The resulting catalytically active ABIL-OH group could leak out from nanocavities. The hot filtration test was also carried out by stopping a standard Knoevenagel condensation after 30 min. Negligible increase in conversion is observed (Fig. 9). These results reveal that the catalytic reaction is truly heterogeneous process.

3.2.3. Size- and shape-selective catalysis

In general, the aromatic aldehydes with electron-donating or electron-withdrawing groups would have an effect on the catalytic performance under homogeneous catalysis, and higher catalytic

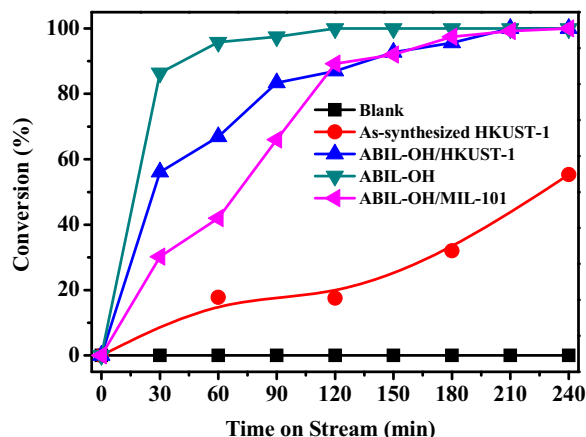


Fig. 6. Kinetic curves of Knoevenagel condensation using different catalyst. Reaction condition: 2 ml toluene, 2 mmol benzaldehyde, 4 mmol malononitrile, reaction temperature = 30 °C, $m_{\text{cat}} = 50 \text{ mg}$ ABIL-OH/HKUST-1, 8 mg ABIL-OH, 73 mg ABIL-OH/MIL-101, respectively.

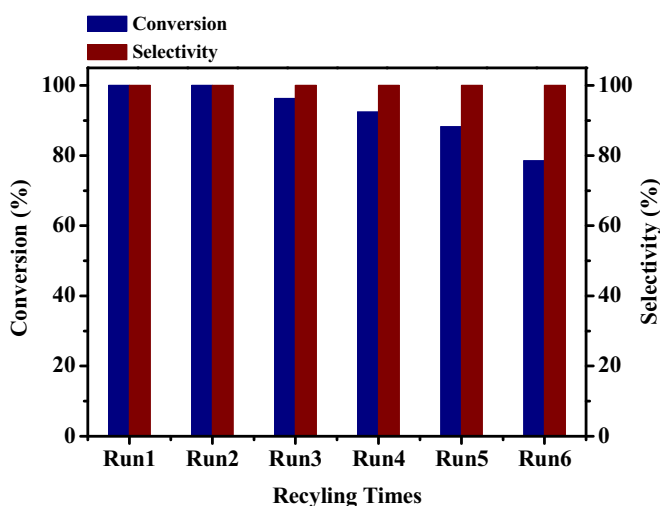


Fig. 8. The recyclability of ABIL-OH/HKUST-1 catalyst for Knoevenagel condensation of benzaldehyde with malononitrile.

activities are obtained for aromatic aldehydes with electron-withdrawing groups. For another thing, however, the aromatic aldehydes with different substituted groups would lead to different molecular size and shape, which might also play an important role on catalytic activities over heterogeneous catalyst. Therefore, we attempted to extend the Knoevenagel condensation reactions to a series of aromatic aldehydes with different substituted groups. The corresponding reactant molecular sizes were calculated by ground state geometric simulation and optimization, as illustrated in **Table 2**. The catalytic activities are depicted in **Fig. 10**.

The Knoevenagel condensation reactions proceed smoothly over homogeneous ABIL-OH organocatalyst. The conversion of 4-(dimethylamino) benzaldehyde (substrate 5) decreases slightly (97%) due to existence of +I (electron donating inductive effect) effect. The rest of all substrates show 100% conversion, but the products selectivity of substrate 2 and 4 are decreased to 82% and 95%, respectively. These results indicate that ABIL-OH organocatalyst exhibits excellent generality for Knoevenagel condensation. Interestingly, it is obvious to note that the increase in reactants sizes have a great influence on the catalytic activities over the ABIL-OH/HKUST-1 heterogeneous catalyst. The smallest benzaldehyde molecule (substrate 1) with dimensions of $6.64 \times 4.64 \text{ \AA}$ shows 100% conversion. The p-chlorobenzaldehyde (substrate 2) with

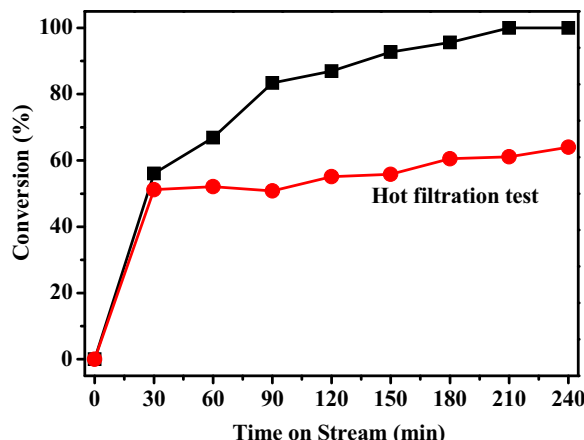


Fig. 9. The hot filtration test over ABIL-OH/HKUST-1 catalysts.

Table 2
The calculation of different molecular size by ground state geometric optimizations and simulation.

Substrate	Aromatic aldehyde	Molecular size ($\text{\AA} \times \text{\AA}$)
1		6.64×4.64
2		7.25×4.64
3		8.12×4.69
4		8.94×4.86
5		9.08×4.85
6		6.65×5.41
7		7.60×6.43
	Hydrogen atom	● Nitrogen atom
	Oxygen atom	● Chlorine atom

dimensions of $7.25 \times 4.64 \text{ \AA}$ demonstrates 82% conversion. The conversions of p-methoxybenzaldehyde and p-isopropylbenzaldehyde (substrate 3 and 4) with molecular dimensions of $8.12 \times 4.69 \text{ \AA}$ and $8.94 \times 4.86 \text{ \AA}$ are decreased to 56% and 48%, respectively. The reactant 4-(dimethylamino) benzaldehyde (substrate 5) with

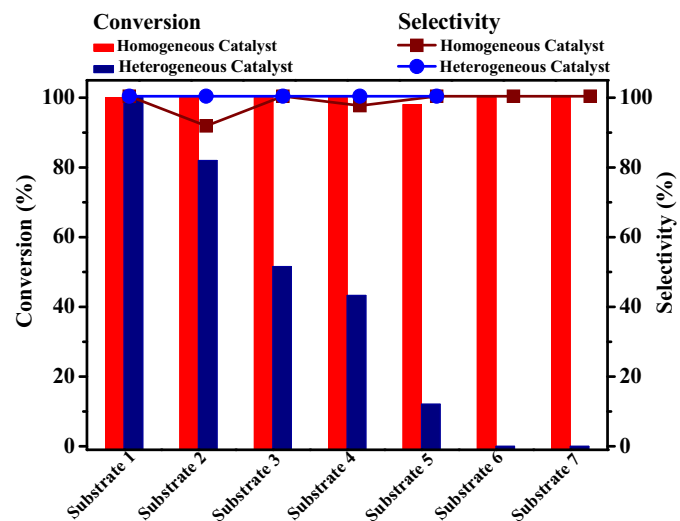


Fig. 10. Results for Knoevenagel condensation of aromatic aldehydes with malononitrile using ABIL-OH/HKUST-1 as catalyst. Reaction condition: 2 ml toluene, 2 mmol aromatic aldehydes, 4 mmol malononitrile, reaction time = 3.5 h reaction temperature = 30°C , $m_{\text{cat}} = 50$ mg ABIL-OH/HKUST-1, 8 mg ABIL-OH, respectively.

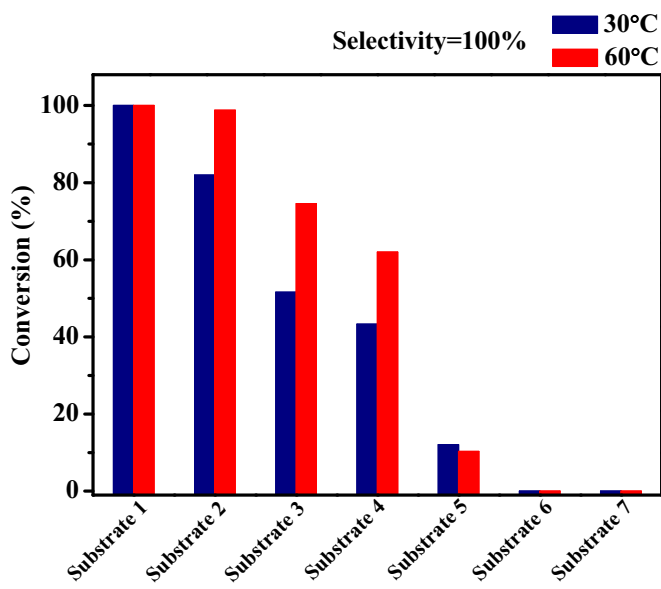


Fig. 11. Knoevenagel condensation of aromatic aldehydes with malononitrile over ABIL-OH/HKUST-1 catalyst under different temperature.

dimensions of $9.08 \times 4.85 \text{ \AA}$ displays only 12.1% conversion. For all of the above aromatic aldehydes substrates, the products selectivity maintains 100%. In addition, there is no any catalytic activity for reactant o-hydroxybenzaldehyde ($6.65 \times 5.41 \text{ \AA}$) and 3-methoxy-4-hydroxybenzaldehyde ($7.60 \times 6.43 \text{ \AA}$), which could be attributed to a difficult rotation and steric factor in confined microenvironment.

N_2 physical adsorption–desorption has demonstrated that the pore size distribution of ABIL-OH/HKUST-1 catalyst is about 0.6–0.8 nm. It is thereby reasonable that the reactants with matched sizes could diffuse smoothly through the nanocavities. Therefore, diffusion of reactants might be an important factor for catalytic activity. Further considering thermodynamics, different reactants must meet certain activation energies over specified catalyst. For this reason, the Knoevenagel condensation was further investigated under higher temperature (Fig. 11). As seen from the figure, the conversions of reactants with matched sizes

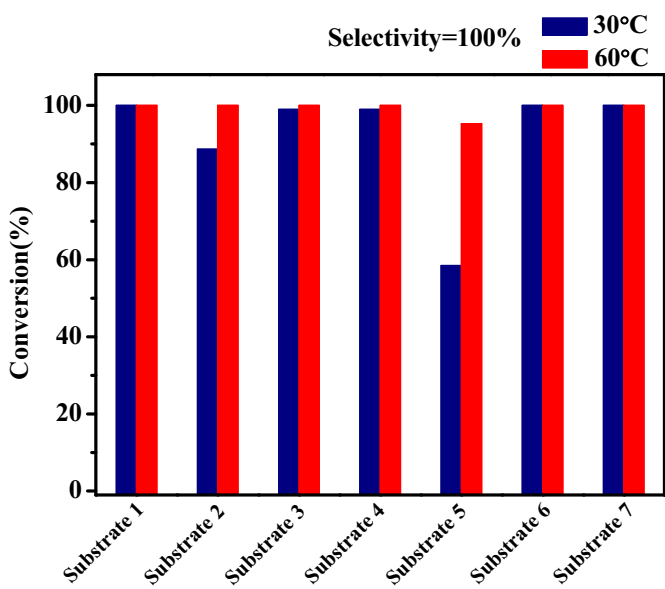


Fig. 13. Knoevenagel condensation of aromatic aldehydes with malononitrile over ABIL-OH/MIL-101 catalyst under different temperature.

(substrates 2, 3, and 4) are increased significantly. From these results, it is supposed that these reactants could diffuse through the nanocavities and catalytic activities are also affected by thermodynamics. However, substrate 5 with larger size has no increase in conversion indicating that diffusion of reactants might be the controlling step in confined microenvironment. In addition, there is still no any obvious catalytic activity for substrate 6 and substrate 7. In this case, the catalytic activities seem to depend on the size and shape of the reactants.

To better discern the molecule size and shape-selective catalysis, another MOFs material with large pore window (12–16 Å) and mesoporous cages (29–34 Å) so-called MIL-101 was employed to immobilize ABIL-OH organocatalyst. The representative 3D pore network was illustrated in Fig. 12. The loading amount of ABIL-OH within MIL-101 nanocages is 0.73 mmol g^{-1} . And it was also tested under the same total number of OH⁻ active species. The corresponding catalytic activities of different aromatic aldehydes are shown in Fig. 13. As expected, conversions of all aromatic aldehydes are improved significantly over ABIL-OH/MIL-101 catalyst, and products selectivity also to maintain 100%. Similarly, the substrate 5 displays lower conversion (58.5%) than others. It is interesting to note that the substrate 6 and substrate 7 show excellent conversions. A reasonable explanation for this result should be that reactant molecules with smaller size ($6.65 \times 5.41 \text{ \AA}$ and $7.60 \times 6.43 \text{ \AA}$) are able to rotate freely and interact with active species inside open mesoporous nanocages. Furthermore, Knoevenagel condensation over ABIL-OH/MIL-101 catalyst was also investigated under higher temperature. It is clearly observed that all aromatic aldehyde exhibit 100% conversions.

In addition, kinetic curve of Knoevenagel condensation between benzaldehyde and malononitrile over ABIL-OH/MIL-101 catalyst was also investigated, as depicted in Fig. 6. Unexpectedly, the initial reaction rate over ABIL-OH/MIL-101 catalyst is slower than that over ABIL-OH/HKUST-1 catalyst before 120 min. And then, both catalytic activity and reaction rate are almost same. This deviant phenomenon could be ascribed to confinement effect. In the confined microenvironment, the benzaldehyde molecule with matched dimensions ($6.64 \times 4.64 \text{ \AA}$) is more favorable to interact with active species.

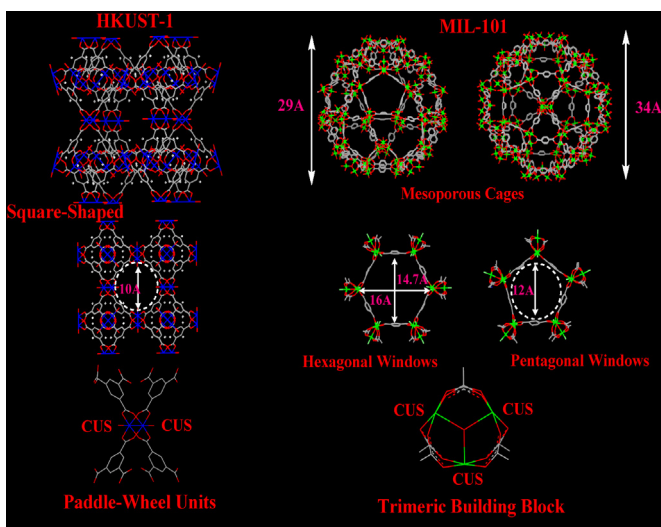
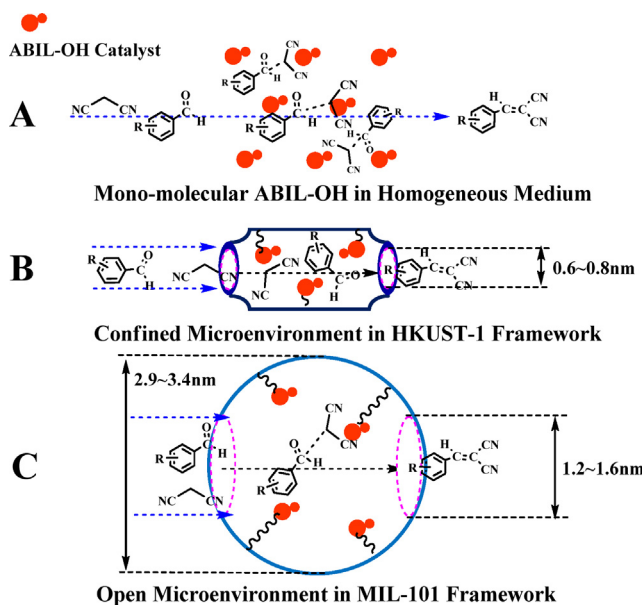


Fig. 12. The three-dimensional (3D) pore network of metal-organic framework HKUST-1 (left) and MIL-101 (right).



Scheme 4. The schematic mechanism in different catalytic microenvironment. (A) Homogeneous ABIL-OH organocatalyst; (B) ABIL-OH/HKUST-1 heterogeneous catalyst; (C) ABIL-OH/MIL-101 heterogeneous catalyst.

Based on the foregoing results and related literatures [25,55,56], it is found that catalytic microenvironment could have a profound effect on Knoevenagel condensation. We propose the catalytic mechanism over different catalyst, as illustrated in Scheme 4. In the case of homogeneous catalysis, the catalytically active species as mono-molecule are dispersed in reactive medium, which is beneficial to interact with reactants. The ABIL-OH organocatalyst exhibits excellent catalytic activity and generality for Knoevenagel condensation. As a consequence, the nature of substituent group might play a critical role. In the confined microenvironment of ABIL-OH/HKUST-1 catalyst, the diffusion of reactants might be controlling steps and play a leading role for Knoevenagel condensation. In other words, the molecular size and shape of reactants could serve as a more important factor than nature of substituent group for Knoevenagel reaction. In open microenvironment, the nature of substituent group (thermodynamics) and diffusion of reactant might be a co-leading role for Knoevenagel condensation.

4. Conclusions

In summary, we demonstrated a novel molecular size- and shape-selective catalyst by immobilization of amino-functionalized basic ionic liquid onto microporous metal-organic framework HKUST-1. The catalytically active groups ABIL-OH are confined inside well-defined HKUST-1 nanocavities via Cu–NH₂ coordination bond. The resulting ABIL-OH/HKUST-1 catalyst shows comparable catalytic activity and enhanced selectivity, and it could be reused at least 5 times. More importantly, the confined microenvironment of ABIL-OH/HKUST-1 catalyst provides distinct size- and shape-selective catalytic properties for discrimination of reactants. The knowledge from this contribution opens up new possibility to design and develop highly active and selective catalyst based on nanoporous metal-organic framework materials. Meanwhile, this strategy would bridge the distance between heterogeneous and homogeneous catalysis by combination of MOFs and task-specific ionic liquid organocatalyst.

Acknowledgments

This work was supported by the National Natural Science Foundation of China (21076031 and 21356001) and Fundamental Research Funds for the Central Universities (DUT12ZD219). Prof. Sang-Eon Park thanks Dalian University of Technology for the “Seasky” professorship.

Appendix A. Supplementary data

Supplementary data associated with this article can be found, in the online version, at <http://dx.doi.org/10.1016/j.apcata.2014.03.041>.

References

- [1] B. Smit, T.L. Maesen, *Nature* 451 (2008) 671–678.
- [2] Y. Shin, J. Liu, L.Q. Wang, Z. Nie, W.D. Samuels, G.E. Fryxell, G.J. Exarhos, *Angew. Chem.* 112 (2000) 2814–2819.
- [3] A. Corma, *J. Catal.* 216 (2003) 298–312.
- [4] T.L. Maesen, R. Krishna, J.M. van Baten, B. Smit, S. Calero, J.M. Castillo Sanchez, *J. Catal.* 256 (2008) 95–107.
- [5] Y. Iwase, Y. Sakamoto, A. Shiga, A. Miyaji, K. Motokura, T.-R. Koyama, T. Baba, *J. Phys. Chem. C* 116 (2012) 5182–5196.
- [6] S. Horike, M. Dinca, K. Tamaki, J.R. Long, *J. Am. Chem. Soc.* 130 (2008) 5854–5855.
- [7] L.G. Qiu, A.J. Xie, L.D. Zhang, *Adv. Mater.* 17 (2005) 689–692.
- [8] A. Dhakshinamoorthy, M. Opanasenko, J. Čejka, H. Garcia, *Catal. Sci. Technol.* 3 (2013) 2509–2540.
- [9] S.M. Cohen, *Chem. Rev.* 112 (2011) 970–1000.
- [10] S.M. Cohen, *Chem. Sci.* 1 (2010) 32–36.
- [11] G. Lu, S. Li, Z. Guo, O.K. Farha, B.G. Hauser, X. Qi, Y. Wang, X. Wang, S. Han, X. Liu, *Nat. Chem.* 4 (2012) 310–316.
- [12] H.-L. Jiang, B. Liu, T. Akita, M. Haruta, H. Sakurai, Q. Xu, *J. Am. Chem. Soc.* 131 (2009) 11302–11303.
- [13] C.-Y. Sun, S.-X. Liu, D.-D. Liang, K.-Z. Shao, Y.-H. Ren, Z.-M. Su, *J. Am. Chem. Soc.* 131 (2009) 1883–1888.
- [14] J. Song, Z. Luo, D.K. Britt, H. Furukawa, O.M. Yaghi, K.I. Hardcastle, C.L. Hill, *J. Am. Chem. Soc.* 133 (2011) 16839–16846.
- [15] A. Yperen-De Deyne, V. Speybroeck, P. Der Voort, *Chem. Commun.* 49 (2013) 8021–8023.
- [16] M.H. Alkordi, Y. Liu, R.W. Larsen, J.F. Eubank, M. Eddaoudi, *J. Am. Chem. Soc.* 130 (2008) 12639–12641.
- [17] R.W. Larsen, L. Wojtas, J. Perman, R.L. Musselman, M.J. Zaworotko, C.M. Vetro-mile, *J. Am. Chem. Soc.* 133 (2011) 10356–10359.
- [18] S.S.-Y. Chui, S.M.-F. Lo, J.P. Charmant, A.G. Orpen, I.D. Williams, *Science* 283 (1999) 1148–1150.
- [19] A. Demessence, D.M. D'Alessandro, M.L. Foo, J.R. Long, *J. Am. Chem. Soc.* 131 (2009) 8784–8786.
- [20] E. Borfecchia, S. Maurelli, D. Gianolio, E. Groppo, M. Chiesa, F. Bonino, C. Lamberti, *J. Phys. Chem. C* 116 (2012) 19839–19850.
- [21] S. Balalaie, M. Sheikh-Ahmadi, M. Bararjanian, *Catal. Commun.* 8 (2007) 1724–1728.
- [22] Y. Kubota, Y. Nishizaki, Y. Sugi, *Chem. Lett.* 29 (2000) 998–999.
- [23] P. Shanthan Rao, R. Venkataratnam, *Tetrahedron Lett.* 32 (1991) 5821–5822.
- [24] S. Saravanamurugan, M. Palanichamy, M. Hartmann, V. Murugesan, *Appl. Catal. A* 298 (2006) 8–15.
- [25] M.B. Ansari, H. Jin, M.N. Parvin, S.-E. Park, *Catal. Today* 185 (2012) 211–216.
- [26] Y. Peng, J. Wang, J. Long, G. Liu, *Catal. Commun.* 15 (2011) 10–14.
- [27] J. Gascon, U. Aktay, M.D. Hernandez-Alonso, G.P. van Klink, F. Kapteijn, *J. Catal.* 261 (2009) 75–87.
- [28] A. Dhakshinamoorthy, M. Opanasenko, J. Čejka, H. Garcia, *Adv. Synth. Catal.* 355 (2013) 247–268.
- [29] M. Opanasenko, A. Dhakshinamoorthy, M. Shamzhy, P. Nachtigall, M. Horáček, H. Garcia, J. Čejka, *Catal. Sci. Technol.* 3 (2013) 500–507.
- [30] R.V. Hangarge, D.V. Jarikote, M.S. Shingare, *Green Chem.* 4 (2002) 266–268.
- [31] D.-Z. Xu, Y. Liu, S. Shi, Y. Wang, *Green Chem.* 12 (2010) 514–517.
- [32] C.P. Mehner, *Chem. Eur. J.* 11 (2005) 50–56.
- [33] M. Valkenberg, W. Hölderich, *Green Chem.* 4 (2002) 88–93.
- [34] H. Li, P.S. Bhadury, B. Song, S. Yang, *RSC Adv.* 2 (2012) 12525–12551.
- [35] Y. Zhang, C. Xia, *Appl. Catal. A* 366 (2009) 141–147.
- [36] Y. Zhang, Y. Zhao, C. Xia, *J. Mol. Catal. A* 306 (2009) 107–112.
- [37] C. Paun, J. Barklie, P. Goodrich, H. Gunaratne, A. McKeown, V. Parvulescu, C. Hardacre, *J. Mol. Catal. A* 269 (2007) 64–71.
- [38] Q. Zhang, J. Luo, Y. Wei, *Green Chem.* 12 (2010) 2246–2254.
- [39] M.N. Parvin, H. Jin, M.B. Ansari, S.-M. Oh, S.-E. Park, *Appl. Catal. A* 413 (2012) 205–212.
- [40] B. Karimi, M. Vafaeenezadeh, *Chem. Commun.* 48 (2012) 3327–3329.
- [41] Y. Shen, Y. Zhang, Q. Zhang, L. Niu, T. You, A. Ivaska, *Chem. Commun.* 33 (2005) 4193–4195.
- [42] S. Guo, S. Dong, E. Wang, *Adv. Mater.* 22 (2010) 1269–1272.

- [43] B. Wu, D. Hu, Y. Kuang, B. Liu, X. Zhang, J. Chen, *Angew. Chem. Int. Ed.* **48** (2009) 4751–4754.
- [44] Q.-X. Luo, M. Ji, M.-G. Lu, C. Hao, J.-S. Qiu, Y.-Q. Li, *J. Mater. Chem. A* **1** (2013) 6530–6534.
- [45] N.A. Khan, Z. Hasan, S.H. Jhung, *Chem. Eur. J.* **20** (2014) 376–380.
- [46] E.D. Bates, R.D. Mayton, I. Ntai, J.H. Davis, *J. Am. Chem. Soc.* **124** (2002) 926–927.
- [47] Z. Zhang, Y. Xie, W. Li, S. Hu, J. Song, T. Jiang, B. Han, *Angew. Chem. Int. Ed.* **47** (2008) 1127–1129.
- [48] C. Prestipino, L. Regli, J. Vitillo, F. Bonino, A. Damin, C. Lamberti, A. Zecchina, P. Solari, K. Kongshaug, S. Bordiga, *Chem. Mater.* **18** (2006) 1337–1346.
- [49] F. Giordanino, P.N. Vennestrom, L.F. Lundsgaard, F.N. Stappen, S.L. Mossin, P. Beato, S. Bordiga, C. Lamberti, *Dalton Trans.* **42** (2013) 12741–12761.
- [50] S. Poulston, P. Parlett, P. Stone, M. Bowker, *Surf. Interface Anal.* **24** (1996) 811–820.
- [51] L. Kundakovic, M. Flytzani-Stephanopoulos, *Appl. Catal. A* **171** (1998) 13–29.
- [52] H. Chen, L. Wang, J. Yang, R.T. Yang, *J. Phys. Chem. C* **117** (2013) 7565–7576.
- [53] A. Dhakshinamoorthy, M. Alvaro, P. Concepcion, H. Garcia, *Catal. Commun.* **12** (2011) 1018–1021.
- [54] K. Schlichte, T. Kratzke, S. Kaskel, *Micropor. Mesopor. Mater.* **73** (2004) 81–88.
- [55] K. Parida, S. Mallick, P. Sahoo, S. Rana, *Appl. Catal. A* **381** (2010) 226–232.
- [56] J. Mondal, A. Modak, A. Bhaumik, *J. Mol. Catal. A* **335** (2011) 236–241.